Embryogenesis in the glass sponge *Oopsacas minuta*: Formation of syncytia by fusion of blastomeres

S. P. Leys,[1,*] E. Cheung,[*] and N. Boury-Esnault[†]

*Department of Biological Sciences CW405, University of Alberta, Edmonton, Alberta, Canada T6G 2E9; †Centre d'Océanologie de Marseille, Université de la Méditerranée, Station marine d'Endoume, UMR-CNRS DIMAR, 6540 rue de la Batterie des Lions, 13007 Marseille, France

Synopsis Sponges (Porifera) are unusual animals whose body plans make interpreting phylogenetic relationships within the group and with other basal metazoan taxa a difficult task. Although molecular approaches have offered new insights, some questions require a morphological approach using detailed ultrastructural or light microscopical studies of developing embryos and larvae. Glass sponges (Hexactinellida) have perhaps the most unusual body plan within the Metazoa because the majority of the tissue of the adult consists of a single giant multinucleated syncytium that forms the inner and outer layers of the sponge and is joined by cytoplasmic bridges to uninucleate cellular regions. Here we have used serial section transmission and high-resolution scanning electron microscopy to examine when syncytia first form in the cave-dwelling glass sponge *Oopsacas minuta*. We confirm that in *O. minuta* blastomeres are separate until the 32-cell stage; cleavage is equal but asynchronous until a hollow blastula is formed. The sixth division yields a collection of variously sized micromeres at the surface of the embryo and large yolk- and lipid-filled macromeres lining the blastocoel. Syncytia then form by the fusion of micromeres to form cytoplasmic bridges with each other and the fusion of macromeres to form the future multinucleated trabecular tissue of the larva and adult sponge. The multinucleated trabecular tissue envelops and forms cytoplasmic bridges with all uninucleate cells, covering the developing larva with a continuous syncytial epithelium. Differentiation of tissues occurs very early during embryogenesis with the separation of uninucleate and multinucleate lineages, but all cells and syncytia are joined by cytoplasmic bridges such that there is cytoplasmic continuity throughout the entire larva. Although glass sponges begin life as a cellular embryo, the unusual mechanism of syncytia formation at such an early stage in development distinguishes this group of animals from their closest multicellular relatives, the Demospongiae. Most important, however, these data lend support to the hypothesis that the original metazoans were cellular, not syncytial.

Introduction

With the rapid progress in molecular techniques, resolving the relationships among basal metazoan phyla is becoming more feasible, but detailed morphological observations of early development are also important for determining ancestral character states of the most basal metazoan groups. The traditional phylogeny of the Porifera, adopted in a recent review of the phylum (Hooper and Van Soest 2002), identifies 3 classes, distinguished by their skeletal morphology, its composition, and its mechanism of deposition: Hexactinellida (commonly called "glass sponges": sponges with a siliceous skeleton secreted intracellularly around a square axial filament), Demospongiae (sponges with a siliceous and/or organic skeleton secreted intra- or extracellularly around a triangular or hexagonal axial filament or with no skeleton), and the Calcarea (sponges with a calcium carbonate skeleton secreted extracellularly within a collagenous sheath, but with no axial filament).

The similarity in "glassyness" of the siliceous skeleton of hexactinellids and demosponges led de Laubenfels (1955) to propose linking a collection of the siliceous sponges in the class Hyalospongiae. A major objection to the combination of these 2 groups into a single class has been the distinct triaxial spicule geometry and square axial filament of hexactinellid sponges (Reid 1963), but it was nevertheless agreed that they could be united at the subphylum level, thus distinguishing the 2 major groupings of sponges as the Silicea and Calcarea (Reid 1957, 1963). Recent analyses of 18s rRNA and protein coding genes also suggest sponges are paraphyletic (Collins 1998; Kruse and others 1998; Zrzavy and others 1998; Borchiellini and others 2001; Medina and others 2001). Despite the relatively weak bootstrap support on these analyses, the

From the symposium "The New Microscopy: Toward a Phylogenetic Synthesis" presented at the annual meeting of the Society for Integrative and Comparative Biology, January 4–8, 2005, at San Diego, California.

[1] E-mail: sleys@ualberta.ca

Integrative and Comparative Biology, volume 46, number 2, pp. 104–117
doi:10.1093/icb/icj016
Advance Access publication February 16, 2006

idea has been expressed quite prominently in the literature because it provocatively suggests that the ancestor of the Cnidaria and other metazoans was a spongelike animal. The name Silicispongia, a term originally proposed by Gray (1867), has been reintroduced to refer to a common clade including Hexactinellida and Demospongiae (Zrzavy and others 1998), and Calcispongia, to refer to calcareous sponges (Borchiellini and others 2001).

The fossil record is limited, but the available evidence does not refute these suggested relationships. Fossils identified as hexactinellid spicules are known from the late Proterozoic (stratigraphically corresponding to the Ediacara Formation of Australia), whereas the first record of demosponge spicules is later in the lower Cambrian (Steiner and others 1993; Reitner and Mehl 1995; Brasier and others 1997). Interestingly, spicules from 2 genera of an extinct group of siliceous sponges known from the Burgess Shale (*Eiffelia* and *Chancelloria*) show intriguing features, including the presence of calcium carbonate. If the analysis is correct, these fossils suggest that all 3 major sponge groups may have arisen from an ancestral stock of siliceous "proto-sponges" (Reid 1963; Botting and Butterfield 2005). Thus, fossil and molecular evidence suggests that siliceous sponges diverged first from a common ancestor and hexactinellids diverged next from other siliceous sponges, that is, that siliceous sponges form a common clade (Müller 1995; Reitner and Mehl 1995, 1996; Collins 1998; Kruse and others 1998; Schütze and others 1999; Mehl-Janussen 2000; Medina and others 2001). Another characteristic supports this conclusion: analysis of chemical biomarkers suggests that siliceous sponges share similar membrane characteristics and microbial communities (Thiel and others 2002).

Morphological data suggest another interpretation of sponge relationships. A detailed study of the living tissue, ultrastructure, and physiology has conclusively demonstrated the largely syncytial structure of hexactinellid sponge tissues. The adult glass sponge is composed of a giant multinucleate tissue, the trabecular syncytium, that stretches from dermal (outer) to atrial (inner) surfaces (Mackie and Singla 1983; Boury-Esnault and De Vos 1988; Reiswig and Mehl 1991; Boury-Esnault and Vacelet 1994; Leys 1995, 1999). This tissue surrounds uninucleate portions of the sponge and is connected to these by cytoplasmic bridges plugged with a unique proteinaceous junction (Mackie 1981; Mackie and Singla 1983). The continuity of this tissue throughout the whole animal allows these sponges, alone among the Porifera, to propagate electrical signals that cause the immediate arrest of the feeding current (Lawn and others 1981; Leys and Mackie 1997).

Knowledge of glass sponge tissue structure prompted the proposed separation of all sponges into 2 subphyla, the Symplasma for sponges with syncytial tissues and the Cellularia for sponges with cellular tissues and either a siliceous or calcareous skeleton (Reiswig and Mackie 1983). A similar proposal by Bidder (1929)—Nuda, sponges without a cellular mesohyl, and Gelatinosa, sponges with a cellular mesohyl—was considered by Reid (1963) but rejected on the grounds that glass sponges likely arose from a common cellular, siliceous choanoflagellate stock rather than 2 separate stocks with and without adhesive material between cells. Reid's argument was based on drawings of a cellular larva in *Farrea sollasii* by Okada (1928), the only hexactinellid for which detailed embryological studies existed. Clearly, further evidence of embryogenesis is needed for this argument.

The reason we know so little about embryogenesis in hexactinellids is that their embryos are difficult to obtain, primarily because of the deep-water habitat of the adults but also because many specimens collected are not reproductive. There is the added complication that fixation techniques with hexactinellids are difficult (Mackie and Singla 1983). The finding in a cave near Marseille, France, of a tiny species of glass sponge that is reproductive year round allowed reexamination of development and confirmed the largely cellular nature of the embryo and larva (Boury-Esnault and others 1999). But in neither Okada's (1928) nor this recent study was it explained exactly how the syncytial tissues of the adult sponge arise.

From both Okada (1928) and Boury-Esnault and colleagues (1999) we know that *F. sollasii* Schulze, 1886, and *Oopsacas minuta* Topsent, 1927, share very similar early development. Cleavage is total and equal, and the 16-cell embryo is a hollow blastula of equally sized cells. Okada (1928) describes the *F. sollasii* embryo as planula-like with 2 cellular layers. The outer layer has up to 3 types of "cell elements," and the inner mass has 2 types of amoeboid cells with numerous yolk granules. The later embryo is nearly spherical, with an outer layer of closely packed cells and a central mass of a clear, transparent, jellylike substance surrounding amoeboid cells that have wandered in from the outer layer. Some of the wandering cells are multinucleate and form spicules, which first appear at the periphery of the inner mass. Others form the collar cells of choanocyte chambers which appear in the center of the embryo.

In *O. minuta* all divisions are also equal until the 32-blastomere stage (Boury-Esnault and others 1999). The sixth cleavage is unequal, resulting in a layer of micromeres on the outside and macromeres on the inside of the hollow blastula. According to these

authors, the micromeres multiply at the surface to make an external flat syncytial layer and a layer of multiciliated cells (Boury-Esnault and others 1999). The macromeres divide to fill up the center of the embryo and form 2 cell types, a type with mostly lipid that remains uninucleate and lies at the future anterior pole of the larva the another type with yolk, which lies at the posterior pole of the larva. The latter type apparently forms a multinucleate tissue and also gives rise to separate multinucleate "cells" that form the spicules.

From these 2 descriptions we understand the glass sponge larva to consist of a complex mixture of uninucleate and multinucleate "cells." It is a difficult combination to comprehend, and it is not clear exactly how multinucleate tissues arise. Here we have reexamined early embryogenesis in *O. minuta* using light, transmission, and scanning electron microscopy with the specific goal of determining when syncytial tissues form during the ontogeny of glass sponges.

Methods

Adult specimens of *O. minuta* were collected in November 2002 at 20 m depth in the 3PP submarine cave near La Ciotat, France (Vacelet and others 1994). Specimens were chipped off the rock at their base into glass containers and transported to the Station Marine d'Endoume in Marseille. Sponges were transferred while still submerged to containers of cold cave seawater and maintained at 12°C. To obtain embryos, whole specimens (3–6 cm long) were cut in half lengthwise and immersed instantly in a cocktail fixative of 1% osmium tetroxide, 2% glutaraldehyde, in 0.45 M sodium acetate buffer (pH 6.4) with 10% sucrose in the final mixture. The fixative was changed after 30 min and sponges were left at 4°C for 2 h. Specimens were rinsed briefly in distilled water and dehydrated to 70% ethanol for transport to the University of Alberta, Canada. Individual embryos (<100 μm in diameter) identified at 120× magnification with an Olympus SZX stereomicroscope were carefully removed from the tissue of adult specimens using forceps. Images of whole embryos were captured using a QI Cam digital monochrome camera and Northern Eclipse software.

Embryos were desilicified in 4% HF in 70% ethanol (en bloc) overnight, then rinsed twice in 70% ethanol and stained in 0.5% uranyl acetate in 70% ethanol (en bloc) for a second night. Finally embryos were dehydrated to 100% ethanol, infiltrated in epoxy (Embed 812) overnight, and embedded. Serial thick sections of 119 embryos were cut with a diamond knife and stained in Richardson's (Richardson and others 1960); images were captured on a Zeiss Axioskop compound microscope using the imaging system described above. Thin sections were collected intermittently through the embryo, stained with lead citrate and viewed in a Phillips (FEI) transmission electron microscope. For scanning electron microscopy, adult sponges were desilicified as described above, dehydrated to 100% ethanol, and fractured in the vial of ethanol in liquid nitrogen, or embryos were removed whole from the adult tissue as described above and dehydrated to 100% ethanol. Specimens were critical-point dried, mounted on aluminum stubs with nail polish, coated with gold, and viewed in a JEOL 6301F field emission scanning electron microscope.

Results

Embryogenesis

Early cleavage in *O. minuta* is total and equal until the 32-cell stage (Fig. 1). The first cleavage divides the oocyte neatly in 2 (Fig. 1A and B). The second cleavage division may be either equatorial or rotational (Fig. 1C and D). Embryos with 6 blastomeres, but not 8, were found, suggesting that early cleavage is asynchronous (Fig. 1E and F). The 16- and 32-cell embryos are hollow blastulas (Fig. 1G–L) whose cells are held together by numerous filopodia that project from their surfaces (Fig. 1L). Although in thick sections the nuclear region of early blastomeres is easily identified (Fig. 1F), a nuclear envelope was not found in thin sections of any blastomere; instead an electron dense region (presumably DNA) in the center of the cell radiates out into the cytoplasm (Fig. 1J). Yolk inclusions are distributed around the nucleus and lipid inclusions are at the periphery of each cell (Fig. 1F, J, and K).

After the fifth cycle (~32-cell stage) cleavage is unequal and results in the division of blastomeres into a collection of irregularly shaped cells surrounding the blastocoel (Fig. 2). Small cuboidal cells 4–6 μm in diameter (micromeres) lie at the outer surface, and large yolk- and lipid-rich cells (macromeres), also very irregular in shape, surround the blastocoel (Fig. 2A–H). Many of the embryos are polarized at this stage; one side of the embryo usually lacks micromeres altogether, whereas the opposite pole has fewer yolk- and lipid-filled macromeres (Fig. 2A–C). Micromeres have distinct nuclei 3–4 μm in diameter with a clear nuclear envelope (for example, Fig. 3A), and some differentiate first a single, and subsequently multiple, cilia (Figs. 2A and 3A). Importantly, all micromeres are connected to each other by cytoplasmic bridges with characteristic hexactinellid "plugged junctions" (Figs. 2H and I and 3A).

Initially, the macromeres still surround a hollow blastocoel, but sections of multiple embryos suggest

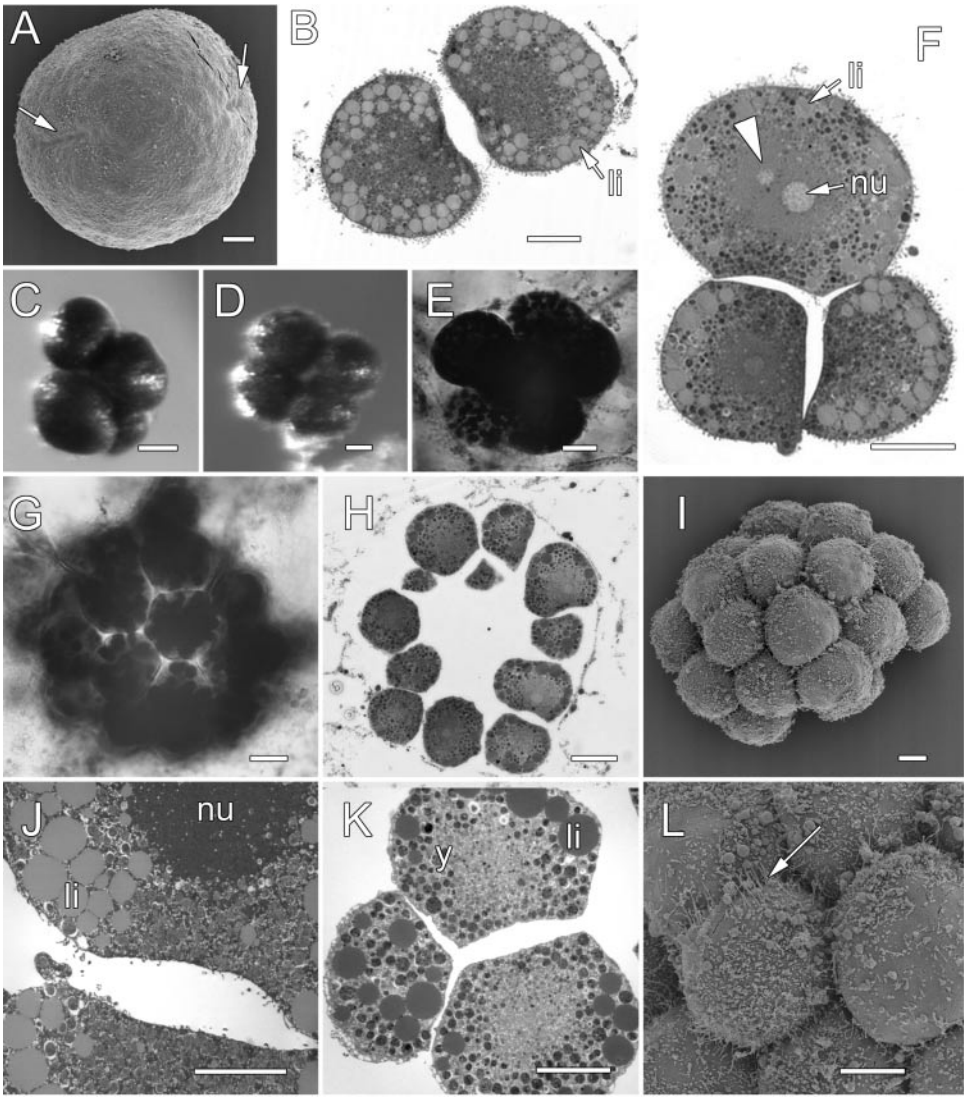

Fig. 1 Early cleavage stages in the development of *O. minuta*. (A) Oocyte showing depressions marking the first cleavage plane (arrows); scanning electron microscopy. (B) 2-cell stage. Blastomeres have numerous filopodia, a dense nuclear region, and large lipid inclusions at the periphery. Thick section of an epoxy embedded embryo. (C and D) Stereomicrographs of 4-cell-stage embryos dissected out of the adult sponge. (C) shows rotational and (D) equatorial cleavage patterns. (E and F) Plastic sections of two 6-cell stage embryos. (E) shows an embryo with dark, lipid inclusions; (F) shows a section through 3 of the 6 cells of another embryo. One of the cells appears to have 2 nuclei (arrow and arrowhead). The fact that epoxy penetrates between the blastomeres suggests there is no cytoplasmic connection between cells at this stage. (G–I, K and L) 16- and 32-cell-stage embryos. (G) and (H) show 2 views of plastic embedded embryos. (I) and (L) are scanning electron micrographs of an embryo dissected out of the parent sponge. (J) is a transmission electron micrograph of the 2 blastomeres from (B). (K) shows a transmission electron micrograph of the blastomeres from the embryo in (H). Blastomeres are uniformly sized and are tenuously held together by vast numbers of filopodia at their surfaces (L, arrow). Scale bars: (A, J, and K), 10 μm; (B–I and L), 20 μm. li, lipid inclusion; nu, nucleus; y, yolk.

that the macromeres become elongate and gradually fill the center of the blastula (Figs. 2A–D and 3B). Once the embryo is solid, lamellipodia extend from the apical surface of the macromeres to envelop the micromeres (Fig. 3B–F), thereby forming the outer epithelium of the embryo. Furthermore, the macromeres also produce filopodia that interdigitate and appear to fuse (Fig. 3C, upper right). All embryos after this stage consist of a single multinucleate tissue—the incipient trabecular reticulum of the future larva and adult sponge—that envelops the micromeres (Figs. 3E, F and 4A–F). Moreover, this macromere-derived

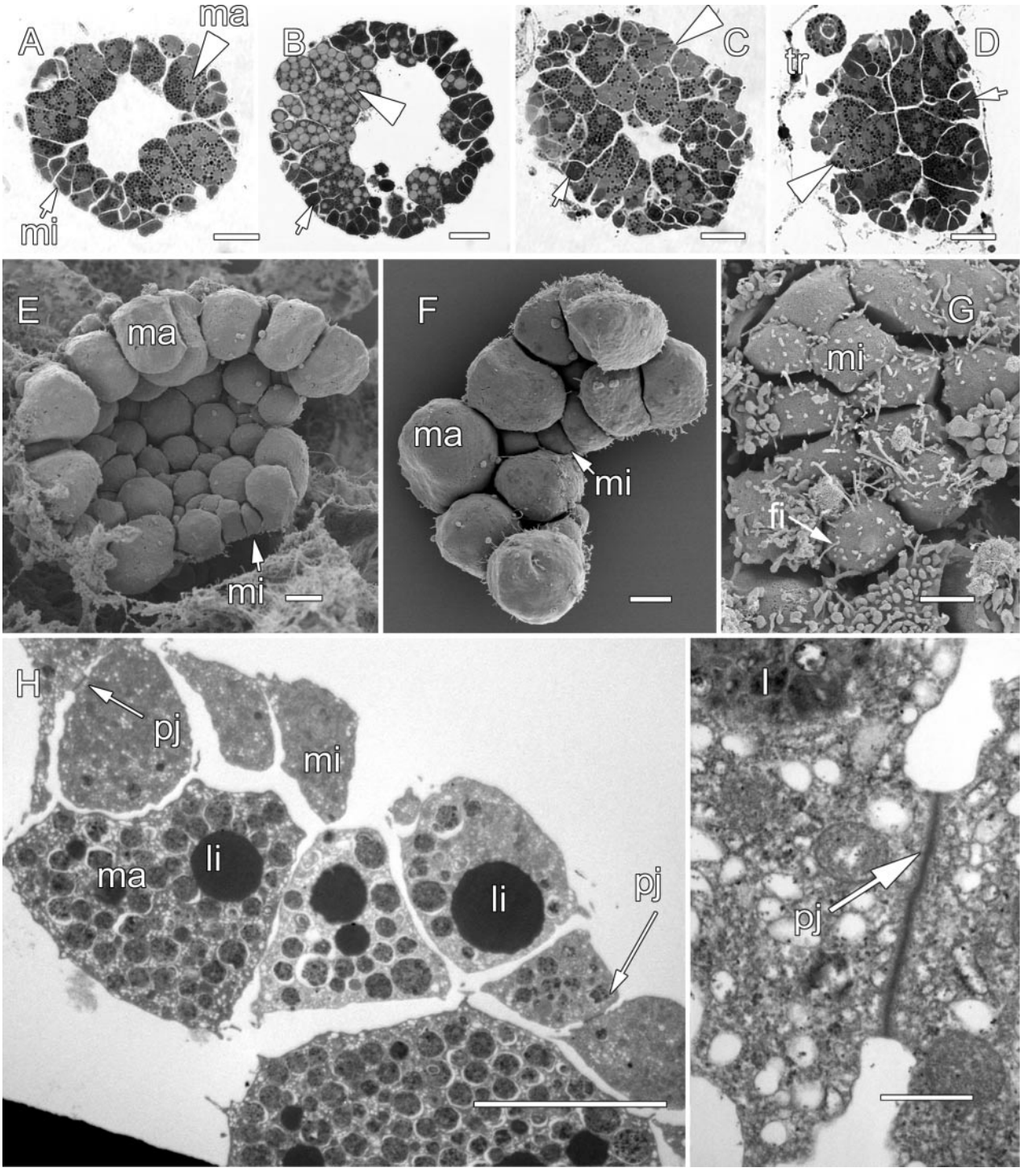

Fig. 2 Fusion of micromeres. All images show embryos after the fifth cleavage, or 32-cell stage. (A–D) Light micrographs of thick epoxy sections; (E–G) scanning electron micrographs; (H and I) transmission electron micrographs. (A–D) show the presumed progression of stages after gastrulation, when micromeres (mi, arrow) are produced at the periphery and macromeres (ma, arrowhead) remain more central as the blastocoel is gradually filled in. (E) and (F) show views of the gastrula from the opened blastocoel; cleavage is not at all equal, and micromeres are wedged in between, and distal to, macromeres. (G) provides a view of the outer surface of an embryo whose micromeres are—similar to the blastomeres of the blastula—covered with small filopodia (fi). (H) and (I) provide detail of the embryo shown in (A). The micromeres are connected to each another by cytoplasmic bridges with a proteinaceous plugged junction (pj). Macromeres (ma) have retained most of the yolk and lipid inclusions. li, lipid inclusion; tr, trabecular tissue.

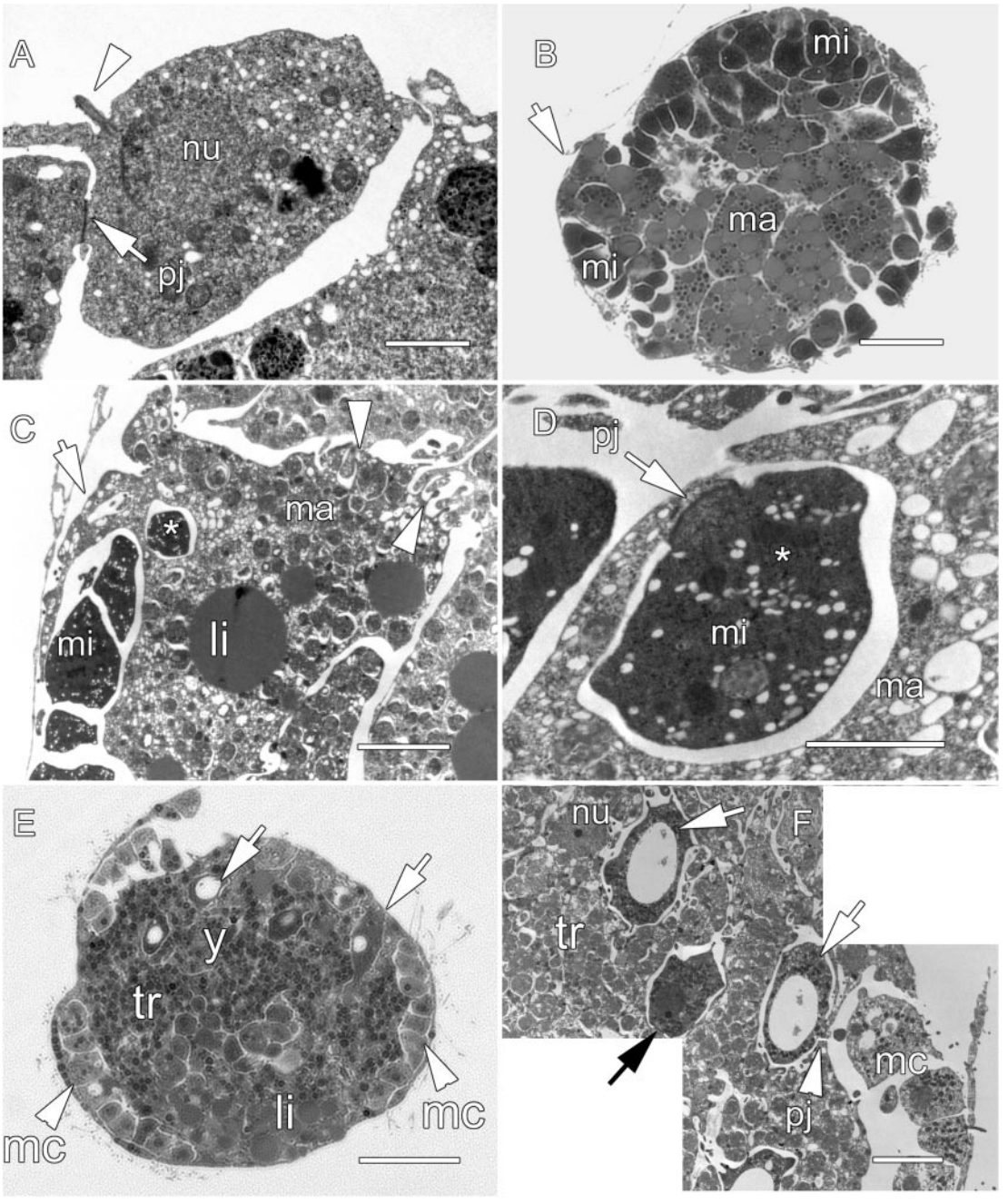

Fig. 3 Fusion of macromeres and formation of syncytia. (A, C, D, and F) Transmission electron microscopy; (B and E) light microscopy of thick epoxy sections. (A) Micromeres from the embryo shown in 2A have already begun to differentiate cilia (arrowhead); these cells are connected to other micromeres by a plugged cytoplasmic bridge (pj). (B) Macromeres (ma) extend around micromeres (mi, arrow) at the surface of the embyo. Note that the surface of some embryos was torn during extraction from the parent tissue. (C) Detail of a region at the surface of the embryo in (B), showing the macromere (ma) extending a lamellipodium (arrow) around micromeres (mi) on the left and forming pseudopodia that intermesh with those of another micromere at the right (arrowheads). (D) Image of the macromere (ma) shown in (C), several sections further into the embryo. The macromere has formed a cytoplasmic bridge with a plugged junction (pj) connecting it to the micromere (mi) marked with an asterisk in (C). (E) An embryo in which the macromeres have completely fused and have enveloped the micromeres within a continuous covering membrane that has torn during removal from the parent sponge. Both multiciliated cells (mc) and sclerocytes (arrows) have already differentiated. The remainder of the embryo consists of a single syncytial trabecular (tr) tissue that contains yolk (y) and lipid (li) inclusions. (F) Detail of the periphery of the embryo in (E), showing that the differentiation of sclerocytes (sc) occurs after multicilated cells (mc). Young sclerocytes have pseudopodia, and may wander through the trabecular tissue (tr), but they are still connected to the trabecular tissue by plugged cytoplasmic bridges (pj). Scale bars: (A, C, and D), 2 μm; (B and E), 20 μm; (F), 5 μm. nu, nucleus.

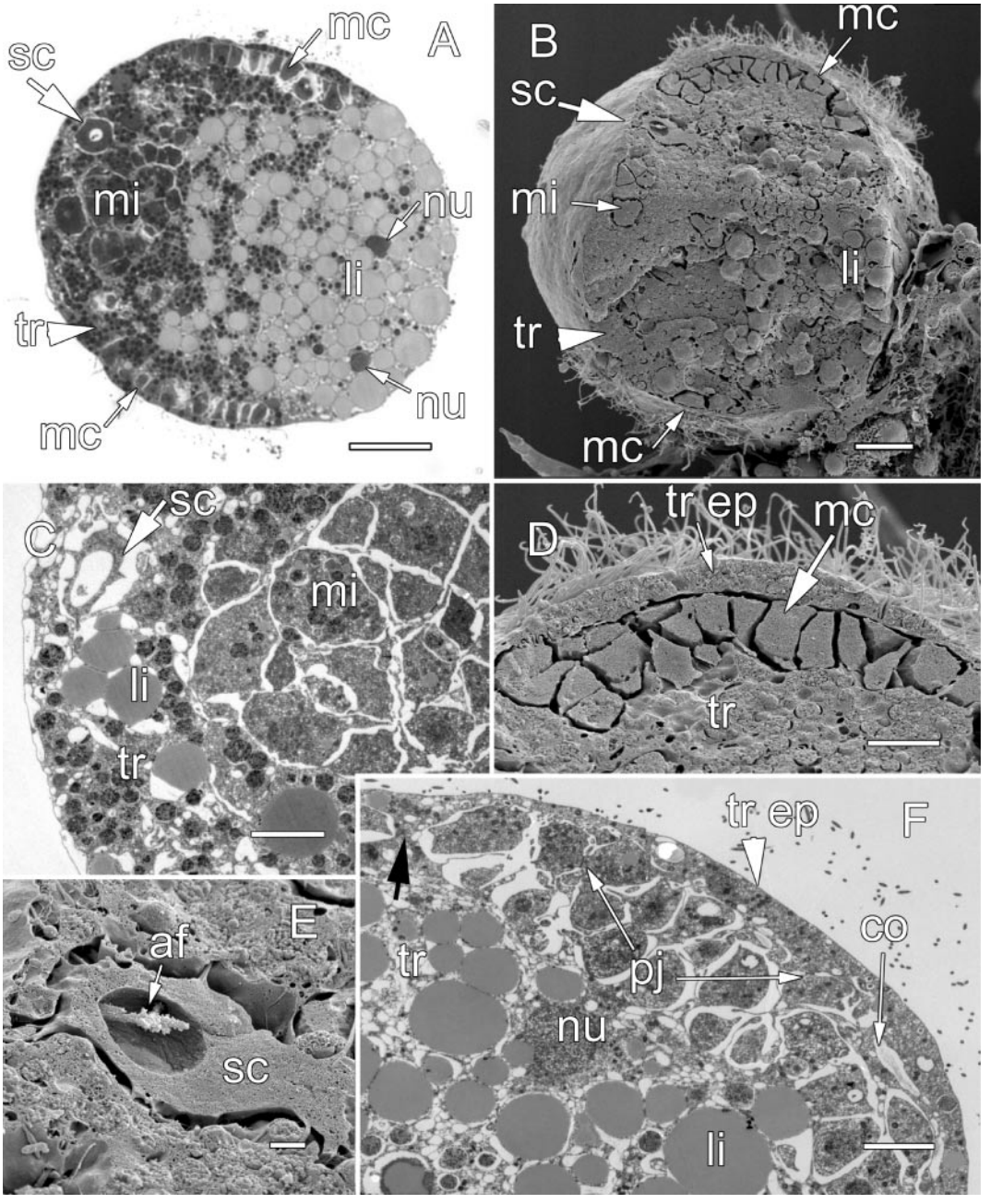

Fig. 4 Early larval differentiation. Images show embryos in which the macromeres have formed a single multinucleated tissue, the trabecular tissue (tr), which has completely covered the micromeres during formation of the embryonic and future larval epithelium (trabecular epithelium, tr ep). (A) Light microscopy of a thick epoxy-embedded section; (B, D, and E) scanning electron microscopy; (C and F) transmission electron microscopy. (A and B) The embryo becomes clearly polarized with the relocation of lipid inclusions (li) to the future anterior pole (right), multiciliated cells (mc) around the equator, and sclerocytes (sc) toward the posterior pole (left). Micromeres (mi) located in the central-posterior portion of the embryo will give rise to the future flagellated chambers. The multinucleate (nu) trabecular tissue (tr) forms more than 70% of the embryo. (C and D) Enlargements of the posterior (C) and lateral (D) regions of the embryos shown in (A) and (B), showing the sclerocytes (sc) and micromeres (mi) cradled within the yolk and lipid-filled (li) cytoplasm of the trabecular tissue (tr). The trabecular tissue forms a continuous syncytial epithelium (tr ep) that encloses the multiciliated cells (mc). (E). An enlargement of the sclerocyte (sc) shown in (B), highlighting the 4-rayed proteinaceous axial filament (af) of the incipient stauractin spicule that remains after desilicification of the specimens. (F) An enlargement of the anterolateral region of the embryo in (A), showing the trabecular tissue (tr) with nuclei (nu) and lipid inclusions (li) that reaches around and envelops (arrow) the multiciliated cells to form the trabecular epithelium (tr ep). Multiciliated cells are connected to each other and to the trabecular tissue by plugged junctions (pj). Collagen (co) has already been deposited in spaces within the trabecular tissue. Scale bars: (A and B), 20 μm; (C, D, and F), 5 μm; (E), 1 μm.

tissue forms cytoplasmic bridges with the micromeres and each of these bridges contains a plugged junction (Fig. 3D).

After it is formed, the trabecular reticulum becomes regionalized, with more yolk at the future posterior pole and more lipid at the future anterior pole (Fig. 3E). Micromeres also differentiate, but at all times they maintain cytoplasmic continuity with the trabecular reticulum and other cells via cytoplasmic bridges. Multiciliated cells form a single band around the equator of the embryo with their cilia projecting through the syncytial epithelium (Figs. 3 E and F and 4A–D). Sclerocytes, spicule-producing cells, produce a square axial filament within a small vacuole while they are still at the periphery of the embryo (Fig. 3F). They develop numerous long pseudopodia and migrate in at the posterior pole, and at the same time the vacuole enlarges with the secretion of silica around the proteinaceous axial filament. The sclerocytes then elongate from the posterior region, and as they extend to the anterior pole they become multinucleate (Figs. 4E and 5A–C). Other micromeres also ingress into the posterior central region, and as the embryo elongates these cells form the choanocyte chambers (Figs. 4C, 5C, and 6C, D). The choanocyte begins as a single nucleated cell with a single flagellum and a collar of microvilli (Fig. 6D), and all such cells are connected to similar cells and to the trabecular tissue by plugged cytoplasmic bridges. Subsequently the portion of the cell containing the collar and flagellum (collar body) becomes separated by a long cytoplasmic bridge from the region with the nucleus. In late embryos the trabecular reticulum envelops and penetrates the small spherical chambers that are formed by collar bodies, but even in the fully developed embryo the chambers lack the bilayered reticulum of the adult sponge and they are not connected to the outside of the embryo (Fig. 6C and D). Spherulous cells are the last cell type to become identifiable in the posterior-central region. These cells contain large spherulous inclusions and are the only cell type in which a cytoplasmic bridge and plugged junction have not been found.

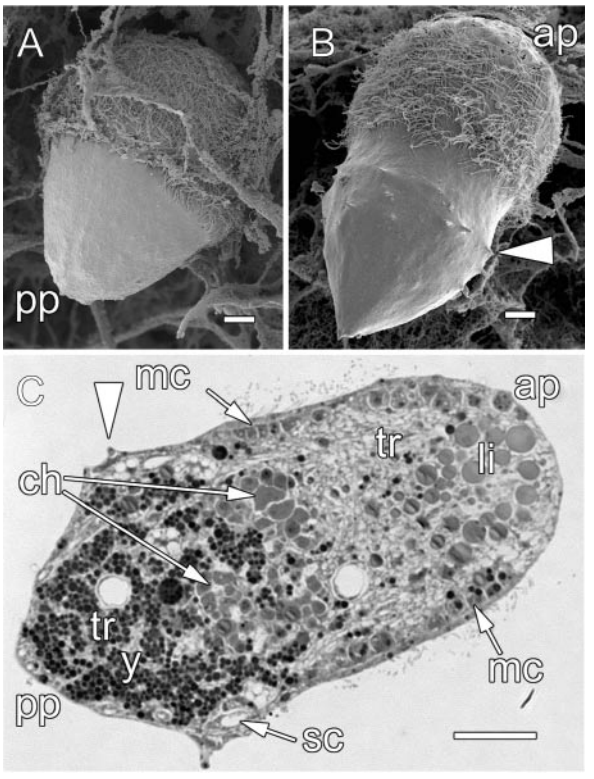

Fig. 5 Late larval differentiation. (A and B) Scanning electron microscopy; (C) light microscopy of an epoxy-embedded thick section. (A and B). The larva begins to take shape by elongating first at the posterior pole (pp, A) and then at the anterior pole (ap, B). As the spicules grow, their transverse rays protrude as points (arrowhead) under the syncytial epithelium. Multiciliated cells form a skirt around the waist of the larva. (C). A section of a larva at the stage shown in (B) reveals projections of spicules (arrowhead), multiciliated cells (mc), lipid inclusions (li) at the anterior pole and yolk inclusions (y) at the posterior pole in the trabecular tissue (tr), and choanocytes (ch) forming early flagellated chambers centrally. Scale bars: (A–C), 10 μm. sc, sclerocytes.

Larval structure

The resulting larva is syncytial, like the adult. It consists of a continuous multinucleate tissue that reaches from anterior to posterior poles, forms the outer epithelium and the bulk of the inner mass, and is connected to cellular components via cytoplasmic bridges (Fig. 5A–C). Multiciliated cells form a belt around the central third of the larva. Their cilia project through the syncytial epithelium (Fig. 6A and B). Flagellated chambers occur in the center-posterior half of the larva but are not connected to a canal system (Fig. 6C and D). Sclerocytes are a thin sheath of multinucleate cytoplasm that surrounds stauractine (4-rayed) spicules whose long rays lie longitudinally from the lipid-dense anterior pole to the yolk-filled posterior at the periphery of the larva (Figs. 5C and 6E). The intersection of the short rays occurs at a point a third of the distance from the posterior pole, and the distal ends of the long rays converge at the posterior pole. Within the trabecular reticulum in the central-posterior portion of the larva lie 4 to 6 choanocyte chambers 10–15 μm in diameter.

The trabecular reticulum surrounds all of the cellular components and extends from anterior to posterior

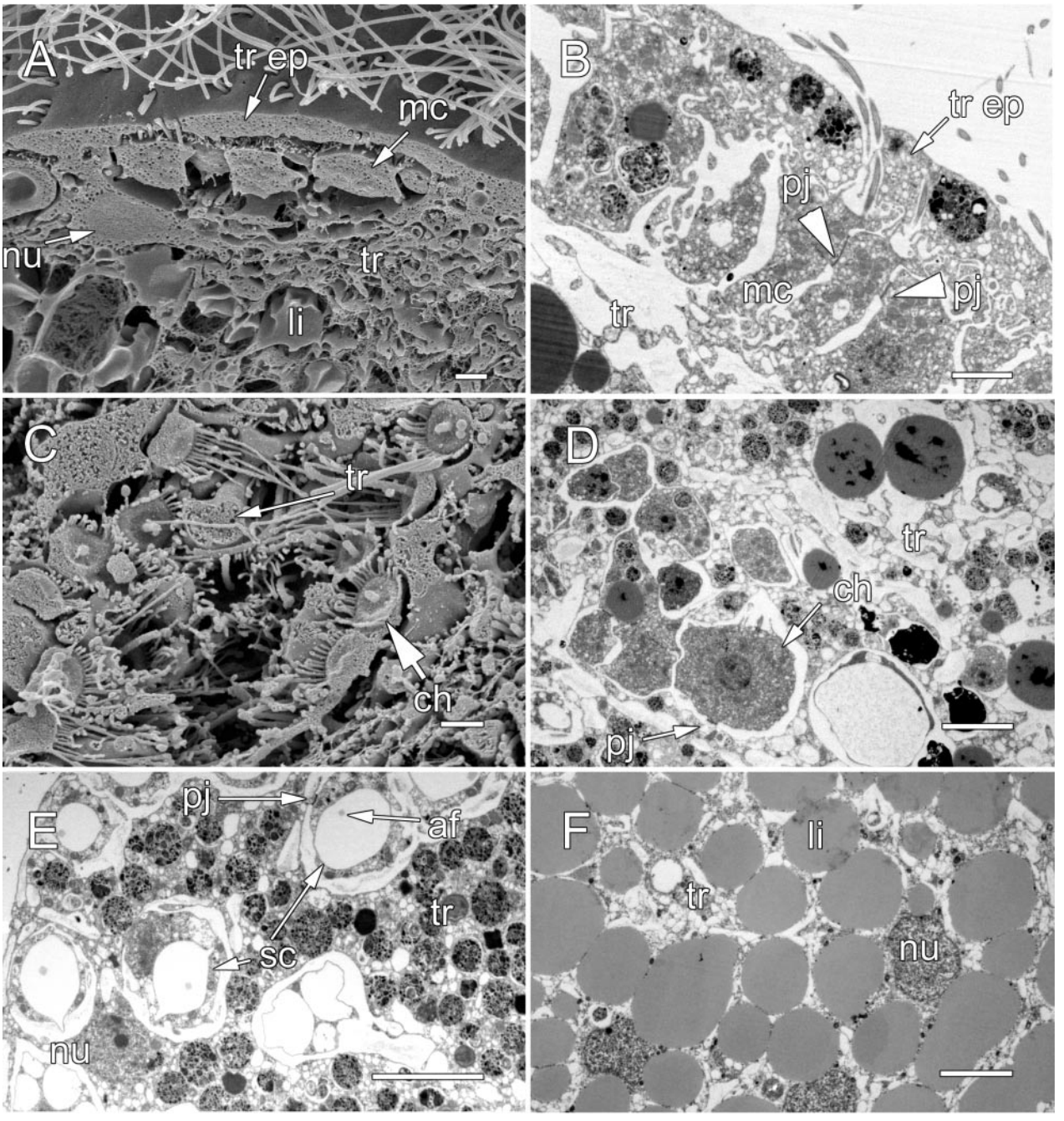

Fig. 6 (A and C) Scanning electron microscopy; (B, D, E, and F) transmission electron microscopy. (A) A fracture across the equator of a larva shows that the reticular network of trabecular tissue (tr) completely surrounds multiciliated cells (mc), whose many cilia pierce the trabecular epithelium (tr ep); li, lipid inclusion. (B) A section of the equivalent regions from (A) shows that multiciliated cells are connected to each other and to the trabecular tissue (tr) by plugged cytoplasmic bridges (pj) and that their cilia are completely surrounded by the trabecular epithelium (tr ep). (C and D) Aspects of the choanocyte chambers in the early larva. Collars and flagella (arrow) are fully formed and arise initially from a nucleated cell (ch) that is connected to the trabecular tissue by a plugged cytoplasmic bridge (pj); they subsequently become branched to form several collars for any given choanocyte. At this early stage the chambers are not yet fully differentiated; choanocytes with nuclei and collar branches arising from choanoblasts lie between strands of the trabecular tissue (tr), but primary and secondary reticula are not yet formed. (E) Differentiated sclerocytes (sc) at the posterior pole of the larva. Sclerocytes (sc), identified by the spicule space and axial filament (af), are separated from the trabecular tissue (tr) by plugged cytoplasmic bridges (pj). (F) A section near the anterior pole shows 3 nuclei (nu) and lipid inclusions (li) within thin strands of the trabecular tissue (tr). Scale bars: (A and C), 1 μm; (B), 2 μm; (D–F), 5 μm.

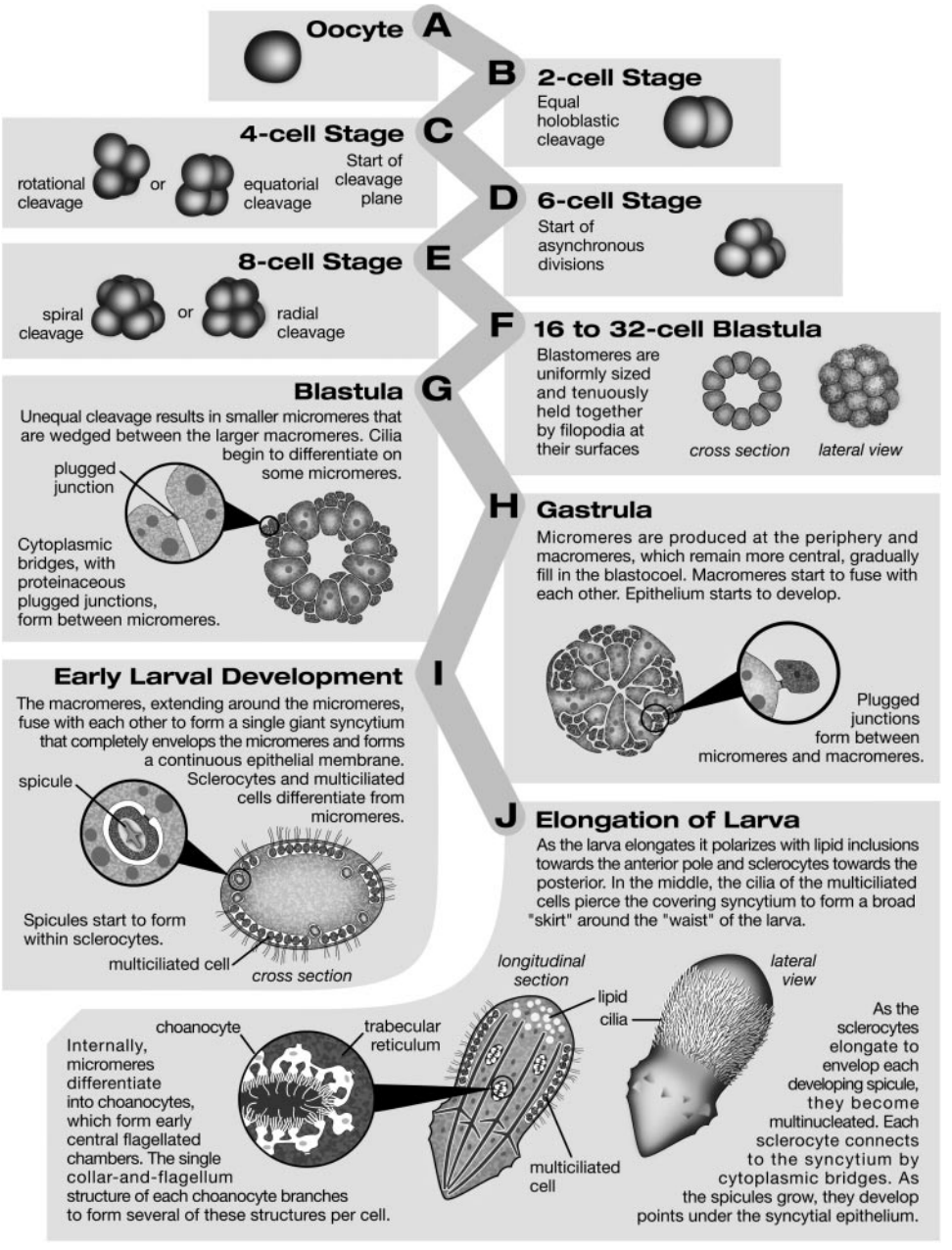

Fig. 7 Diagrams of the stages in the early development of *O. minuta* as detailed in Table 1.

pole. At the anterior pole the trabecular tissue consists of thin strands with a little yolk, and large spherical lipid inclusions (Figs. 5C and 6). Toward the equator and posterior pole, portions of the trabecular reticulum are thicker, with many small yolk inclusions (Figs. 5C and 6E). Fine strands of this syncytial tissue, interlaced with sheets of collagen (Fig. 6A, B, D, and E), are continuous throughout the larva; there are no membrane boundaries between lipid- and yolk-filled regions.

The stages in early development are summarized in Figure 7 and Table 1.

Discussion

Ultrastructural study of early development in *O. minuta* has revealed 2 new findings. First, plugged cytoplasmic bridges form between micromeres soon after these cells arise. Second, we report that the syncytial tissue of the larva and of the adult is formed by the fusion of the yolk- and lipid-filled macromeres. At the time these cells fuse, they envelop the micromeres, creating an amoeboid syncytial tissue. Furthermore, this tissue then forms cytoplasmic bridges with all the former micromeres. The result is a fully

Table 1 Sequence of events during the early development of *O. minuta* as diagrammed in Figure 7

Stage	Event
A–F	Cleavage
A	Oocyte
B	2-cell stage, equal holoblastic cleavage
C	4-cell stage, rotational or equatorial cleavage
D	6-cell stage, start of asynchronous divisions
E	8-cell stage, "spiral" or "radial" cleavage
F	16- to 32-cell blastula
G–H	Gastrulation
G	>32 cell gastrula 1
	Formation of micromeres
	Differentiation of cilia on micromeres
	Formation of the first plugged junctions between micromeres
H	Infiltration of the blastocoel
	Formation of the embryonic and larval epithelium
	Formation of plugged junctions between micromeres and macromeres
	Start of fusion of macromeres
I–J	Early larval development
I	Complete fusion of macromeres
	Formation of a single giant syncytium
	Differentiation of sclerocytes
J	Elongation of the larva
	Formation of larval spicules
	Differentiation of choanocytes and formation of larval flagellated chambers

cytoplasmically interconnected embryo and larva (Fig. 6). First and foremost, however, these results confirm that syncytial glass sponges and their larvae arise from cellular embryos.

Formation of syncytia

Glass sponge embryos have long been described as being cellular, as have their larvae. The principal difference in our findings from the studies by both Okada (1928) and Boury-Esnault and others (1999) is that although the early embryo is clearly cellular, the gastrula and late embryo are largely syncytial, not cellular.

Serial thick section and thin section transmission electron microscopy allows us to identify key features of glass sponge development such as cytoplasmic bridges in the early micromeres, but the static images do not tell us how the bridges form. Although the bridges could form by incomplete cytokinesis, no micromeres were found in the process of division in any of the 119 embryos serially sectioned. Also, because all the ciliated micromeres in the fully differentiated larva are connected by cytoplasmic bridges, it is assumed that the bridges must arise by fusion of the micromeres after they have formed. All bridges are filled by the proteinaceous plugged junction characteristic of hexactinellid sponges, and although no plugs in the process of being formed were found, it is assumed that plugs arise from the Golgi apparatus, as occurs in aggregates and adult sponges (Pavans de Ceccatty and Mackie 1982; Mackie and Singla 1983), and are then inserted into the cytoplasmic bridge.

Two pieces of evidence strongly suggest that the plugs within these junctions are indeed protein insertions within cytoplasmic bridges as described by Mackie and Singla (1983; reviewed in Leys 2003b) and not locally juxtaposed membranes of distinct cells with membrane proteins such as form a gap junction. First, some extremely large plugs (up to 5 μm) appear to form a barrier that severs the halves of an otherwise continuous cytoplasmic unit (Leys 2003a). Second, cytoplasmic bridges that link newly formed micromeres in the embryo are long and show clear continuity of the plasma membrane of the 2 "cells" through the bridge (for example, Fig. 2H and I).

Cellular differentiation and gastrulation

The early differentiation of the blastomeres into micromeres and macromeres separates the future cellular and syncytial lineages during early development in *O. minuta*. The micromeres give rise to the multiciliated cells that the larva swims with, to the collar cells of the larva's nonflagellated chambers, and also to the multinucleate sclerocytes. The macromeres, and not the micromeres, form the outer epithelium of the larva, and this epithelium is continuous with the multinucleate trabecular tissue that runs throughout the embryo. The early separation of sclerocytes from multiciliated cells and collar bodies (branched choanocytes) supports an early distinction of ciliated and skeletogenic cell lines such as is thought to exist in many sponges—a feature that has been suggested to demonstrate the common ancestry of metazoans (Minchin 1909; Borojevic 1970; reviewed in Leys 2004).

As in other Porifera, the processes that occur during reaggregation of dissociated tissue appear to be analogous to those that occur during embryogenic development (Wilson 1907; Brien 1937; Curtis 1962; Borojevic and Lévi 1965; Korotkova 1970; Bagby 1972; Van de Vyver and Buscema 1981). Fusion of macromeres in the embryo is remarkably similar to the fusion of dissociated portions of the trabecular

tissue seen during in vitro reaggregation experiments on another glass sponge, *Rhabdocalyptus dawsoni* (Pavans de Ceccatty 1982; Leys 1995). Viewed with video microscopy, the formation of syncytia during reaggregation begins with the interaction of lamellipodial membranes for a brief period (~15 min), followed by the almost "instant" fusion of membranes (5 min) and subsequent continuity of cytoplasm, seen by the streaming of cytoplasm between the 2 formerly separate pieces. Thin sections of such aggregates show that they contain the multinucleated tissue that is wrapped around—and has cytoplasmic bridges with—cellular components.

The mechanism by which the outer epithelium forms is to our knowledge unique in the Metazoa. Earlier work claimed that gastrulation occurs by delamination when the micromeres form at the periphery of the embryo (Boury-Esnault and others 1999). However, we now suggest that epithelialization of the embryo by the syncytial tissue could be considered to be the moment of gastrulation, as it results in placing the future larval (and adult) epithelium on the outside and moving the future feeding (pumping) cells, choanocytes, inward, as in some hydroid cnidarians (Cherdantsev and Krauss 1996). This process could be construed as a type of epiboly. Interestingly, the orientation of these 2 layers—epithelium and pumping/feeding cells—does not invert at metamorphosis in the glass sponge, as it does in most demosponges (S.P.L., manuscript in preparation).

Implications for basal metazoan phylogeny

What can we infer from the development of glass sponges about relationships among major sponge clades? As glass sponges are cellular during early development, it is most likely that they derived from a cellular stock of siliceous organisms, as perceived by Reid (1963). Given their basal position within the Metazoa, the broader impact of this finding is that the ancestral metazoan was cellular, not syncytial as has been sometimes advocated in the past (Hadzi 1953). This finding also does not support the proposed separation of cellular and syncytial sponges into subphyla Symplasma and Cellularia (Reiswig and Mackie 1983). Because cleavage patterns and modes of gastrulation can be evolutionarily modified (sometimes even within the same genus), fusion of blastomeres on its own could be considered a modification of the types of gastrulation found in other sponges. Nonetheless, the fact that no other animal (including other sponges) forms syncytial tissues in this way or is largely constructed of syncytial tissues does distinguish the group. In both demosponges and calcareous sponges, early embryos may have multinucleate blastomeres (Franzen 1988; Saller 1988), as is the case in select groups of many other metazoans (Gilbert and Raunio 1997), but to the best of our knowledge, glass sponge embryos present the only case in which individual blastomeres fuse to form multinucleate tissues.

Although we might imagine that molecular sequence data in the end will provide the "final word" on basal metazoan phylogenies, for the moment deep branching points remain difficult to resolve (see, for example, Rodrigo and others 1994; Manuel and others 2003). Morphological data is also limited, but glass sponges have enough unusual characteristics to make firm decisions as to higher taxonomy difficult. They share with demosponges a siliceous skeleton (for example, Sandford 2003) and similar cells in the larva that begin silica deposition (Leys 2003a). They differ from other siliceous sponges in having spicules with cubic (6-rayed) symmetry and a square proteinaceous axial filament, and from all other sponges (and most animals) in forming syncytial tissues by fusion of blastomeres early during development, in lacking contractile tissues and motile cells (amoebocytes), in possessing perforate plugged junctions (a junction most similar to algal pit plugs; Pueschel 1989) (Reiswig and Mackie 1983), and in the unusual organization of their cytoskeleton, which functions in intrasyncytial nutrient transport (Leys 1995).

Siliceous sponges likely share a common cellular, siliceous ancestor, but the 2 groups diverged from each other very long ago. At present there are insufficient data to support the separation of Hexactinellida from Demospongiae and Calcispongiae at the subphylum level, or to unify them completely with Demospongiae in a clade Silicea. We opt to retain their distinction in the class Hexactinellida until further data can conclusively sway the argument.

Acknowledgements

This article has benefited from useful criticism by R. D. Burke, G. O. Mackie, H. M. Reiswig, and A. Collins. We thank C. Jalong, J. Vacelet, and N. Lauzon for help collecting specimens and the director and staff at the Station Marine d'Endoume, where portions of this work were carried out.

References

Bagby RM. 1972. Formation and differentiation of the upper pinacoderm in reaggregation masses of the sponge *Microciona prolifera* (Ellis and Solander). J Exp Zool 180:217–44.

Bidder GP. 1929. Sponges. In: Encylopaedia Britannica. 14th ed. New York: Cox. 254–61.

Borchiellini C, Manuel M, Alivon E, Boury-Esnault N, Vacelet J, Le Parco Y. 2001. Sponge paraphyly and the origin of Metazoa. J Evol Biol 14:171–9.

Borojevic R. 1970. Différenciation cellulaire dans l'embyogénèse et la morphogenèse chez les spongiaires. Zool Soc Lond 25:467–90.

Borojevic R, Lévi C. 1965. Morphogenèse expérimentale d'une éponge à partir de cellules de la larve nageante dissociée. Z Zellforsch 68:57–69.

Botting JP, Butterfield NJ. 2005. Reconstructing early sponge relationships by using the Burges Shale fossil *Eiffelia globosa*, Walcott. Proc Natl Acad Sci USA 102:1554–9.

Boury-Esnault N, De Vos L. 1988. *Caulophacus cyanae*, n. sp., une éponge hexactinellide des sources hydrothermales: biogéographie du genre *Caulophacus* Schulze, 1887. Oceanologica Acta 8:51–60.

Boury-Esnault N, Efremova S, Bézac C, Vacelet J. 1999. Reproduction of a hexactinellid sponge: first description of gastrulation by cellular delamination in the Porifera. Invertebr Reprod Dev 35:187–201.

Boury-Esnault N, Vacelet J. 1994. Preliminary studies on the organization and development of a hexactinellid sponge from a Mediterranean cave, *Oopsacas minuta*. In: van Soest RWM, van Kempen TMG, Braekman J, editors. Sponges in time and space: proceedings of the Fourth International Porifera Congress. Rotterdam: A.A. Balkema. p 407–16.

Brasier MD, Green O, Shields G. 1997. Ediacaran sponge spicule clusters from southwestern Mongolia and the origins of Cambrian fauna. Geology 25:303–6.

Brien P. 1937. La réorganisation de l'éponge après dissociation par filtration et phénomènes d'involution chez *Ephydatia fluviatilis*. Arch Biol 48:185–268.

Cherdantsev VG, Krauss YA. 1996. Gastrulation in the marine hydroid *Dynamena pumila*: an example of evolutionary anticipation based on developmental self-organization. Evol Theory Rev 11:89–98.

Collins AG. 1998. Evaluating multiple alternative hypotheses for the origin of Bilateria: an analysis of 18S rRNA molecular evidence. Proc Natl Acad Sci USA 95:15458–63.

Curtis ASG. 1962. Pattern and mechanism in the reaggregation of sponges. Nature 196:245–8.

de Laubenfels MW. 1955. Porifera. In: Treatise on invertebrate paleontology: part E, ed. RC Moore. Lawrence: Geological Society of America and University of Kansas Press, p 21–122, Figs. 14–89.

Franzen W. 1988. Oogenesis and larval develoment of *Scypha ciliata* (Porifera, Calcarea). Zoomorphology 107:349–57.

Gilbert R, Raunio AM. 1997. Embryology: constructing the organism. Sunderland, MA: Sinauer Associates.

Gray JE. 1867. Notes on the arrangement of sponges, with descriptions of some new genera. Proc Zool Soc London p 492–558.

Hadzi J. 1953. An attempt to reconstruct the system of animal classification. Syst Zool 2:145–54.

Korotkova GP. 1970. Regeneration and somatic embryogenesis in sponges. Zool Soc Lond 25:423–36.

Kruse M, Leys SP, Müller IM, Müller WEG. 1998. Phylogenetic position of the hexactinellida within the phylum Porifera based on the amino acid sequence of the protein kinase C from *Rhabdocalyptus*. J Mol Evol 46:721–8.

Lawn ID, Mackie GO, Silver G. 1981. Conduction system in a sponge. Science 211:1169–71.

Leys SP. 1995. Cytoskeletal architecture and organelle transport in giant syncytia formed by fusion of hexactinellid sponge tissues. Biol Bull (Woods Hole) 188:241–54.

Leys SP. 1999. The choanosome of hexactinellid sponges. Invertebr Biol 118:221–35.

Leys SP. 2003a. Comparative study of spiculogenesis in demosponge and hexactinellid larvae. Microsc Res Tech 62:300–11.

Leys SP. 2003b. The significance of syncytial tissues for the position of the Hexactinellida in the Metazoa. Integ and Comp Biol 43:19–27.

Leys SP. 2004. Gastrulation in sponges. In: Stern C, editor. Gastrulation: from cells to embryo. Cold Spring Harbor: Cold Spring Harbor Press. p 23–31.

Leys SP, Mackie GO. 1997. Electrical recording from a glass sponge. Nature 387:29–31.

Mackie GO. 1981. Plugged syncytial interconnections in hexactinellid sponges. J Cell Biol 91:103a.

Mackie GO, Singla CL. 1983. Studies on hexactinellid sponges: I. Histology of *Rhabdocalyptus dawsoni* (Lambe, 1873). Philos Trans R Soc Lond Biol Sci 301:365–400.

Manuel M, Borchiellini C, Alivon E, Le Parco Y, Vacelet J, Boury-Esnault N. 2003. Phylogeny and evolution of calcareous sponges: monophyly of Calcinea and Calcaronea, high level of morphological homoplasy, and the primitive nature of axial symmetry. Syst Biol 3:311–33.

Medina M, Collins AG, Silberman J, Sogin ML. 2001. Evaluating hypotheses of basal animal phylogeny using complete sequences of large and small subunit rRNA. Proc Natl Acad Sci USA 98:9707–12.

Mehl-Janussen D. 2000. Schwämme in der fossilen Uberlieferung Zbl Geol Paleont Teil ll 1–2:15–26.

Minchin EA. 1909. Sponge-spicules: a summary of present knowledge. Ergebnisse und Fortschritte der Zoologie 2: 171–274.

Müller WEG. 1995. Molecular phylogeny of Metazoa (Animals): monophyletic origin. Naturwissenschaften 82:321–9.

Okada Y. 1928. On the development of a hexactinellid sponge, *Farrea sollasii*. J Fac Sci Imp Univ Tokyo 4:1–29.

Pavans de Ceccatty M. 1982. In vitro aggregation of syncytia and cells of a Hexactinellida sponge. Dev Comp Immunol 6:15–22.

Pavans de Ceccatty M, Mackie G. 1982. Genèse et évolution des interconnexions syncytiales et cellulaires chez une éponge Hexactinellide en cours de réagrégation après dissociation in vitro. C R Acad Sci Paris 294:939–44.

Pueschel CM. 1989. An expanded survey of the ultrastructure of red algal pit plugs. J Phycol 25:626–36.

Reid REH. 1957. On Hexactinellida, "Hyalospongea," and the classification of siliceous sponges. J Paleontol 31:282–6.

Reid REH. 1963. Hexactinellida or Hyalospongea. J Paleontol 37:232–43.

Reiswig HM, Mackie GO. 1983. Studies on hexactinellid sponges: III. The taxonomic status of Hexactinellida within the Porifera. Phil Trans R Soc Lond B Biol Sci 301:419–28.

Reiswig HM, Mehl D. 1991. Tissue organization of *Farrea occa* (Porifera, Hexactinellida). Zoomorphology 110:301–11.

Reitner J, Mehl D. 1995. Early paleozoic diversification of sponges: new data and evidences. Geol Palaont Mitt Innsbruck 20:335–47.

Reitner J, Mehl D. 1996. Monophyly of the Porifera. Verh Naturwiss Ver Hamburg 36:5–32.

Richardson KC, Jarett L, Finke EH. 1960. Embedding in epoxy resins for ultrathin sectioning in electron microscopy. Stain Technol 35:313–23.

Rodrigo AG, Bergquist PR, Bergquist PL, Reeves RA. 1994. Are sponges animals? An investigation into the vagaries of phylogenetic inference. In: van Soest RWM, van Kempen TMG, Braekman J, editors. Sponges in time and space. Rotterdam: A.A. Balkema. p 47–54.

Saller U. 1988. Oogenesis and larval development of *Ephydatia fluviatilis* (Porifera, Spongillidae). Zoomorphology 108:23–8.

Sandford F. 2003. Physical and chemical analysis of the siliceous skeletons in six sponges of two groups (Demospongiae and Hexactinellida). Microsc Res Tech 62:336–55.

Schütze J, Krasko A, Custodio MR, Efremova SM, Müller IM, Müller WEG. 1999. Evolutionary relationships of Metazoa within the eukaryotes based on molecular data from Porifera. Proc R Soc Lond B Biol Sci 266:63–73.

Steiner M, Mehl D, Reitner J, Erdtmann BD. 1993. Oldest entirely preserved sponges and other fossils from the Lowermost Cambrian and new facies reconstruction of the Yangtze platform (China). Beliner Geoviss Abh 9:293–329.

Thiel V, Blumenberg M, Hefter J, Pape T, Pomponi S, Reed J, Reitner J, Wörheide G, Michaelis W. 2002. A chemical view of the most ancient metazoa: biomarker chemotaxonomy of hexactinellid sponges. Naturwissenschaften 89:60–6.

Vacelet J, Boury-Esnault N, Harmelin J. 1994. Hexactinellid Cave, a unique deep-sea habitat in the scuba zone. 41:965–73.

Van de Vyver G, Buscema M. 1981. Capacités morphogènes des cellules d'éponges dissociées. Ann Soc R Zool Belg 111:9–19.

Wilson HV. 1907. On some phenomena of coalescence and regeneration in sponges. J Exp Zool 5:245–58.

Zrzavy J, Mihulka S, Kepka P, Bezdek A. 1998. Phylogeny of the Metazoa based on morphological and 18S ribosomal DNA evidence. Cladistics 14:249–85.